
Article:
Moon, E.M. orcid.org/0000-0002-1779-8587, Ogden, M.D. orcid.org/0000-0002-1056-5799, Griffith, C.S. et al. (2 more authors) (2017) Impact of chloride on uranium(VI) speciation in acidic sulfate ion exchange systems: Towards seawater-tolerant mineral processing circuits. Journal of Industrial and Engineering Chemistry, 51. pp. 255-263. ISSN 1226-086X

https://doi.org/10.1016/j.jiec.2017.03.009

Impact of chloride on uranium(VI) speciation in acidic sulfate ion exchange systems: Towards seawater-tolerant mineral processing circuits

*Ellen M. Moon,[a,b] Mark D. Ogden,[c,b] Christopher S. Griffith,[b] Abigail Wilson[b,d] and Jitendra P. Mata[e,b]

[a]Southern Cross GeoScience, Southern Cross University, PO Box 157, Lismore, NSW 2480, Australia.
[b]ANSTO Minerals, Australian Nuclear Science and Technology Organisation, Locked Bag 2001, Kirrawee D.C., NSW 2232, Australia.
[c]Department of Chemical and Biological Engineering, The University of Sheffield, Mappin Street, Sheffield S1 3JD, U.K.
[d]Engineering and Capital Programs, Australian Nuclear Science and Technology Organisation, Locked Bag 2001, Kirrawee D.C., NSW 2232, Australia.
[e]Australian Centre for Neutron Scattering, Australian Nuclear Science and Technology Organisation, Locked Bag 2001, Kirrawee D.C., NSW 2232, Australia.

*Corresponding author: ellen.moon@scu.edu.au, +61 2 6626 9544

Submitted to the *Journal of Industrial and Engineering Chemistry*
Date 24 October 2016
Revised manuscript submitted 25 February 2017

ABSTRACT

Using X-ray absorption spectroscopy, we have identified the mechanism by which chloride impacts the extraction of U(VI) by a weak base anion exchange resin from acidic sulfate solutions. The amount of chloride present affects U(VI) speciation both in the feed solutions and adsorbed by the resin, and we find three distinct U(VI) species taken up by the resin across the salinity gradient, directly corresponding to changes in levels of U(VI) extraction. These findings are integral to the effective design of mineral processing circuits incorporating seawater – a cheaper and more sustainable water source than fresh water.

GRAPHICAL ABSTRACT

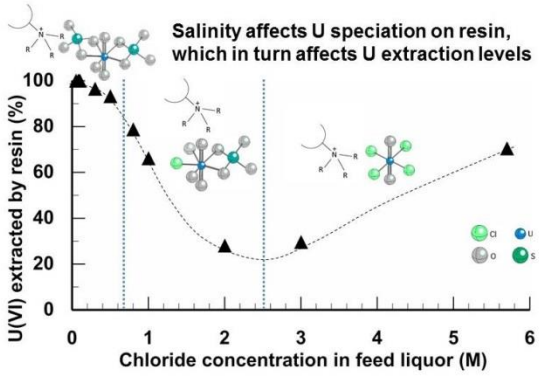

KEY WORDS

uranium; mineral processing; ion exchange; EXAFS; saline.

1. INTRODUCTION

Uranium represents the major fuel source for nuclear energy. In 2014, nuclear power generated 2410.4 TWh of electricity worldwide, 11.1 % of the total global electricity production [1]. The International Atomic Energy Agency estimates this figure will rise to between 2992 and 7771 TWh by 2050 [1]. To accommodate this increased demand for processed uranium, there is continuing need to develop more efficient and cost effective strategies to separate uranium from aqueous streams, both uranium mineral processing streams, and radioactive wastewater streams. Key to effective separation and extraction strategies is a thorough understanding of the uranium speciation before, during and after separation.

The processing of uranium ores with sulfuric acid provides a number of reasons to extend our understanding of uranium speciation in acidic sulfate systems to those in which chloride is also present. There are geochemical drivers: For example, the mobility of uranium in subsurface environments can be heavily dependent on the pH and activity of ligands present in wastewaters (i.e. tailings ponds and mine drainage sites), which are often highly acidic, with high sulfate concentrations [2,3]. Where the surrounding waters are naturally saline, such as borewaters, or seawater, the speciation of uranium may deviate from the typical uranyl sulfate complexes expected, and current thermodynamic data may not be able to predict uranium mobility [4]. There are also industrial drivers: The provision of freshwater for uranium processing circuits is not straight forward, especially in arid areas such as the interior of South Australia, where the world's largest uranium deposit is located [5,6]. There is significant potential for the uranium mining industry to reduce processing costs, and transition to more sustainable water sources, by modifying their processing circuits to accommodate saline process water such as borewater or seawater.

Salinity, however, is known to have a deleterious impact on conventional hydrometallurgical processes used for uranium separation and extraction [7,8]. Chloride concentrations of less than 0.1 M in the feed liquor streams have been shown to reduce uranium extraction by up to 20% [7,9]. Anion exchange resins are routinely used in the uranium processing industry, especially for feed liquor streams containing low uranium concentrations. Weak base anion exchange resins in particular, containing tertiary or secondary amine functional groups, show good selectivity for uranium over impurities, a lower susceptibility to the impact of chloride [10] and have been proposed for use in the extraction of uranium from sulfuric acid liquor streams with elevated chloride concentrations [10,11]. However, a survey of the literature indicates that the chemical mechanisms underpinning the reduced uranium extraction in the presence of chloride has not been extensively studied. In particular, it is not clear to what extent the reduced uranium uptake is due to competition with the chloride anion for surface sites on the resin, or the influence of chloride on uranium speciation. Further, the relationship between the aqueous U speciation, and the speciation of U on the resin surface, is not understood. This is crucial for determining the

mechanism by which chloride impacts ion exchange circuits. Until the underpinning chemistry is understood, it will be difficult to determine how best to adapt current circuits, or design improved circuits, to tolerate saline water.

To the authors' knowledge, there are no studies concerning the speciation of U(VI) in mixed sulfate-chloride media. However, there have been a number of studies concerning the aqueous speciation of U(VI) in chloride and sulfate media separately. In acidic sulfate solutions, there is no consensus over the speciation of U(VI). Some authors have reported that the major species of U(VI) is the $UO_2(SO_4)_3^{4-}$ anion [12-14], whereas others, using spectroscopy and density function theory (DFT), have reported that the major species is the neutral ion $UO_2(H_2O)_3(SO_4)$ and the anion $UO_2(H_2O)(SO_4)_2^{2-}$ [15-17] and indeed, that in solution, 5-fold coordination in the UO_2^{2+} equatorial plane is much more likely than 6-fold coordination [17]. Whether the sulfate is coordinated monodentately or bidentately (and thus the number of aquo ligands in the equatorial plane) seems to depend on the ratio between sulfate and uranyl, with a high $[SO_4^{2-}]/[UO_2^{2+}]$ ratio i.e. 5-600 favouring bidentate complexation [16,18,19] and a low ratio (i.e. < 3) favouring monodentate complexation [16,20,21]. In acidic chloride media, where $0 < [Cl^-] < 3$ M, the U(VI) speciation has been shown using X-ray absorption spectroscopy (XAS) to be dominated by the $UO_2(H_2O)_5^{2+}$ cation with a contribution from $UO_2(H_2O)_4Cl^+$ cation [22,23].

To the authors' knowledge, there has only been one spectroscopic study concerning U(VI) uptake by an anion exchange resin, and this was from chloride media (10 M $[Cl^-]$). Using X-ray absorption spectroscopy (XAS), Allen et al. showed that the speciation of U(VI) on the surface of a strong base resin was $[UO_2Cl_4]^{2-}$, which differed from that identified in the feed solution $[UO_2(H_2O)Cl_4]^{2-}$[22].

Synchrotron-based XAS is a powerful tool that probes the average local coordination geometry of an element of interest within a sample, and as such can help identify the uranium speciation in both the feed liquor and on the resin surface. This study aims to provide a spectroscopic insight into the mechanisms by which chloride affects U(VI) speciation in sulfate-based acidic liquor streams under saline conditions, and subsequent uptake by ion exchange resins. Batch adsorption experiments will be used to quantify U(VI) extraction as a function of chloride concentration, and X-ray absorption spectroscopy will provide the identity of the U(VI) species in solution and taken up by the resin.

2. EXPERIMENTAL

2.1 Resin preparation

2.1.1 Batch experiments

Dowex Monophere 77 is a macroporous tertiary amine anion exchange resin with a polystyrene divinyl benzene (PS-DVB) matrix. Its properties are described in Table 1, and its functionality represented in Figure S1. The presence of both weak base and strong base functionality was determined experimentally

via the Harland method [24]. Resins were pre-treated with 20 bed volumes of 1 M H_2SO_4 in a column at 5 BV h^{-1} to convert to the sulfate form. Resins were then stored in an airtight container in 18.2 MΩ deionised water and adjusted to pH 1.6 with concentrated H_2SO_4.

2.1.2 Synchrotron samples

In order to make the resin suitable for presentation to the synchrotron beam (and avoid artefacts associated with the packing of small spheres), conditioned resin (sulfate form) was dried at 40 °C in an oven for 24 hours. It was then ground with a pestle and mortar into a fine powder.

2.2 Batch extractions from sulfate media

2.2.1 Batch experiments

AR grade reagents and 18.2 MΩ deionised water were used throughout the experiments. The simulant feed (pH 1.6) was prepared at $[SO_4^{2-}]$ = 0.25 M (using H_2SO_4), $[UO_2^{2+}]$ = 0.004 M (using a sulfate-based UO_2^{2+} stock solution of 100 g/L U) and at varying Cl^- concentrations (using NaCl). Small volumes of the feed solutions were retained for synchrotron analysis. All batch extractions were carried out as single contacts with the contact of 2 mL of resin with 50 mL of aqueous simulant feed, as a function of chloride concentration. The resin and aqueous feed were allowed to equilibrate for a period of 24 h at room temperature (21 °C) on an orbital shaker.

2.2.2 Synchrotron samples

Dry resin powder (0.1 g, approximately 0.1 mL)) was contacted with 2.5 mL of feed solution in a 10 mL vial and allowed to equilibrate for a period of 24 hrs at room temperature (21 °C) on an orbital shaker. At 100 % adsorption this equated to a resin sample containing 2.5 wt. % uranium, which is sufficient for EXAFS data acquisition. After 24 hours, the sample was centrifuged at 3000 g for 10 minutes. The supernatant was decanted and retained for analysis, and the resin (a wet paste) was loaded directly into XAS sample holders and sealed with Kapton tape.

2.2.3 Distribution behaviour

The extraction percentage was determined by difference (using eqn. 1) and the concentrations of the individual metal ions determined by either ICP-MS (U) or ICP-OES (S, Cl).

$$E_{\%} = (C_i - C_{aq})/C_i \times 100 \quad (1)$$

Where C_i is the initial metal concentration before contact and C_{aq} is the concentration of the metal ion in the aqueous phase after contact with the resin. pH measurements for solutions were determined using a silver/silver chloride reference electrode calibrated to from pH 1-10 using buffers. At higher acid

concentrations [H^+] were determined by titration and verified by chloride concentration via ion selective electrode analysis. Error was determined by triplicate measurement in aqueous feed solution concentrations prior to contact.

2.3 X-ray absorption spectroscopy

2.3.1 EXAFS data collection

EXAFS fluorescence spectra of the U L3-edge (17.166 keV) were collected at the XAS beamline at the Australian Synchrotron in Victoria, Australia. During data collection, storage ring energy was 3.0 GeV and the beam current was approximately 200 mA. Samples were held in a cryostat at roughly 20 K throughout the data collection process. XAS data were collected from up to 10 scans using a Canberra 100-element Ge solid-state detector. Before data collection, a series of XANES and EXAFS scans was performed on test solution and resin samples to monitor potential U(VI) photo-reduction and X-ray beam damage on the sample. Results indicated no photo-reduction or visible drying of the sample after 10 EXAFS scans to k = 16 $Å^{-1}$. Resin samples were presented to the X-ray beam as a thick paste held in a 1.5 mm-thick Teflon slide with a 4 x 7 mm sample slot. Kapton tape was used either side of the Teflon slide to seal the pastes in and minimize drying. Solution samples were also held within Teflon slides with the same dimensions, again sealed with Kapton tape. All samples were flash frozen in liquid nitrogen before being placed inside the cryostat for data collection. Solution samples were checked for the formation of ice crystals by monitoring the fluorescence detector output for signs of diffraction lines or rings before data collection began.

2.3.2 EXAFS data analysis

XAS data reduction was performed using Viper [25] and PySpline [26]. Viper was used to calibrate from monochromator position (millidegrees) to energy (eV), to deglitch data and to average multiple spectra from individual samples. PySpline was used to perform background subtraction. The pre-edge was fitted to a linear function and the post-edge background to two 3rd-order and two 2nd-order polynomial segments. U EXAFS data were fitted in EXCURV98 [27]. The phase-shifts and potentials were calculated in the small atom (plane-wave) approximation and the phase-shift functions used in the curve fitting were derived by ab initio methods in EXCURV98 using Hedin–Lundqvist potentials [28] and von Barth ground states. All spectra were fitted in k-space and no Fourier filtering was performed during the data analysis. Typical errors associated with EXAFS modelling over the k-range used here are 15 % and 25 % for first and second shell coordination numbers, respectively, ± 0.02 and 0.05 Å for first and second shell distances, respectively, and 15 % and 25 % for first and second shell Debye-Waller factors (DWFs), respectively [27].

Multiple scattering was allowed for as coded in EXCURV98. Multiple scattering calculations require specification of the full three dimensional structure of the U coordination environment (i.e., bond angles in addition to bond lengths). This was done using hypothetical model complexes with C_1 symmetry (Fig. 1 & 2). The number of independent data points (N_{ind}) was determined using Stern's rule [29] as $2\Delta k\Delta R/(\pi+2)$ where Δk and ΔR are the range in k- and R-space actually fitted [30]; as such, $N_{ind} = 23$. Initial complexes were constructed using parameters derived from previous EXAFS investigations into uranium-chloride and uranium-sulfate solution coordination [16,22,23]. Complexes were built in three dimensions, atom by atom, until the addition of another atom failed to improve the fit (as determined by the R-factor) by more than 5 %.

For the resin samples, a total of 19 parameters were refined for the U-*bis*-sulfato species (EF, 7 U-O distances, 2 U-S distances, 9 DWF's; Fig. 1a), 11 parameters for the U-*tetra*-chloro species (EF, 2 U-O istances, 4 U-Cl distances, 6 DWF's; Fig. 1b), and 15 parameters for the mixed U-chloro-sulfato species (EF, 6 U-O distances, 1 U-Cl distance, 1 U-S distance, 8 DWF's; Fig. 1c). Fits to all spectra were also generated using a linear combination of the optimized U-*bis*-sulfato and U-*tetra*-chloro complexes (section 3.2.1) as coded in EXCURV98. The linear combination was performed over k-range 3.5–15 $Å^{-1}$ with a linear combination of the k^3-weighted Chi(k) for the two complexes. In the linear combination, only EF and relative site occupancies were optimized. In all fits $N_{ind} > N_{pars}$.

For the aqueous samples, we refined a total of 10 parameters for the U-*bis*-chloro species (EF, 3 U-O distances, 2 U-Cl distances, 5 DWF's; Fig. 2a), and 19 parameters for the mixed U-chloro-sulfato species (EF, 6 U-O distances, 1 U-Cl distance, 2 U-S distance, 9 DWF's; Fig. 2b). In all fits $N_{ind} > N_{pars}$.

Fit quality was assessed using the EXAFS R-factor (as coded in EXCURV98) and the EXAFS Fit Index [31], with an absolute index of goodness of fit given by the reduced Chi^2 function as coded in EXCURV98 [27]. Further details on the goodness of fit parameters are given in the Electronic Supplementary Information.

3. RESULTS

3.1 Batch extraction studies

The extraction results for uranium adsorption as a function of chloride concentration at pH 1.6 are given in Figure 3. The negative impact of increasing Cl^- concentration on U(VI) uptake by the resin is clear. Below 0.5 M Cl^-, extraction was >90 %, but by 2 M Cl^-, it dropped to ~30 % extraction. Interestingly, U(VI) extraction then steadily increased up to 5.8 M Cl^- to ~70 %. Competition with Cl^- ion uptake could account for the behaviour up to 2 M Cl^-, but it is unlikely to explain the subsequent increase in U(VI) extraction from 3-6 M [Cl^-]. This change in behaviour suggests a change in U(VI) speciation on the resin surface, perhaps to a species for which the tertiary amine resin surface sites have a higher affinity than

214 Cl^- ions. X-ray absorption spectroscopy, which provides the local coordination geometry around a central
215 atom (i.e. U) is the ideal tool to investigate this possible change in speciation.
216
217 3.2 U L3-edge X-ray absorption spectroscopy
218 3.2.1 EXAFS of U(VI) bound to the resin surface
219 EXAFS data and fits for the U(VI) adsorbed resin samples are shown in Figure 4. EXAFS fits are
220 summarized in Tables S1, S2 and S3 in the electronic supplementary information.
221 Upon inspection of the EXAFS data, two 'end member' samples were identified: R1, the resin
222 exposed to a 0.24 M SO_4^{2-} feed solution free from chloride, which likely represented some form of
223 'U(VI)-sulfato' surface complex; and R7, the resin exposed to a 5.8 M Cl^- U(VI) feed solution, which
224 likely represented some form of 'U(VI)-chloro' surface complex. Model complexes were constructed in
225 the EXCURV98 program using parameters (bond lengths and angles, and coordination numbers)
226 identified by previous XAS studies of typical U(VI)-chloride and sulfato solution species [16,23]. Model
227 complexes were built up atom by atom, shell by shell, until subtle iterations of the structural parameters
228 produced good fits to the EXAFS data.
229 For resin sample R1, fitting showed that the U first shell coordination environment consisted of 2
230 O at 1.76 and 1.81 Å. The second shell coordination environment consisted of 5 O at 2.41-2.52 Å, with
231 the U third shell coordination environment consisting of 2 S at 3.08-3.15 Å. These distances and
232 coordination environment are consistent with other U(VI) surface complexes identified by EXAFS
233 spectroscopy [32,33] as well U(VI) solution complexes present in solutions with a 'high' $[SO_4^{2-}]/[UO_2^{2+}]$
234 ratio ($[SO_4^{2-}]/[UO_2^{2+}] > 5$) [15] which is the characteristic of the liquor contacted with the resin. Note that
235 the longest U-O distance represents an oxygen from bound water [33]. The resulting complex can
236 therefore be described as a U-*bis*-sulfato species with both sulfate groups coordinated in a bidentate
237 fashion with U (Fig. 1a). As often occurs, the range of U-O distances and small DWF's of 2nd shells may
238 be an artefact of fitting the five O's to five distinct shells.
239 For the U complex in resin sample R7, the U first shell coordination environment consisted of 2
240 O at 1.79 and 1.75 Å. The U second shell coordination environment consisted of 4 Cl at 2.68-2.73 Å, with
241 no U third shell coordination environment discernible. These distances are consistent with other U(VI)
242 complexes identified by EXAFS spectroscopy [22,23]. The resulting complex can therefore be described
243 as a U-*tetra*-chloro species (Fig. 1b). Again, the small range of U-Cl distances and small DWF's of 2nd
244 shells may be an artefact of fitting the four Cl's to four distinct shells. A fifth Cl atom was not required:
245 The fit using 4 Cl's was very good (R = 17.6), and the addition of a fifth Cl actually lowered the goodness
246 of fit. A U(VI)-*tetra*-chloro species on the resin is consistent with the findings of Allen et al. [22].

A visual comparison of the EXAFS and Fourier transforms of the EXAFS for the 'end-member' resin samples (R1 and R7) and spectra for the other resin samples shows R2 and R3 bear a close resemblance to R1, and that samples R5 and R6 closely resemble R7. To fit R2-6, three approaches were compared: 1) Fitting with an optimised version of either the R1 or R7 complex, 2) Fitting with a linear combination of the R1 and R7 complexes, and 3) Fitting with a 'mixed' sulfato-chloro complex. The results of the three fitting approaches are presented in Table 2. They are described by the goodness of fit parameter, R, for which $R < 30$ represents a good fit, and $R < 20$ represents a very good fit. For the linear combination fit, the goodness of fit parameter, R, is presented alongside the relative proportions of the two components of the linear combination, the U-*bis*-sulfato complex used to fit sample R1, and the U-*tetra*-chloro complex used to fit sample R7.

The fitting for R1, R2, R3, R6 and R7 proved straightforward, with R2 and R3 being fit with optimised versions of the R1 U-*bis*-sulfato complex, and R6 with an optimised version of the R7 U-*tetra*-chloro complex. Optimisation allows for subtle changes in bond lengths and Debye-Waller factors to better fit the individual resin data, but without changing the overall coordination geometry. Fits are presented in Figure 4 and Tables S1 and S2.

The fitting of R4 and R5 was less straightforward. Linear combinations of the complexes used to fit R1 and R7 proved to be an acceptable fit, but a much better fit (both statistically and visually) was achieved by using a mixed sulfate-chloro complex. A number of mixed complexes were constructed and compared to the data: A complex containing 1 bidentate sulfate and 3 chlorides provided a bad fit and was discounted. Further complexes containing 1 or 2 monodentate sulfates, plus a mixture of chlorides and aquo ligands also provided bad fits and were discounted. Two further complexes (the first containing 1 bidentate sulfate, 2 chlorides and an aquo ligand; and the second containing 1 bidentate sulfate, 1 chloride and 2 aquo ligands) provided equally good fits (both statistically and visually). The main difference between these complexes is their charge: $[UO_2Cl_2SO_4(H_2O)]^{2-}$ is more negatively charged than $[UO_2ClSO_4(H_2O)_2]^-$. These complexes were identified in 1 and 2 M $[Cl^-]$ (samples R4 and R5 respectively), which is the region across which the U extraction dropped significantly (see Figure 3). Competition with chloride uptake has previously been proposed as an explanation for this drop in U extraction [7] and competition would most likely exist with another -1 charged anion. Given that the EXAFS fits were equal for both species, we hypothesise that the $[UO_2ClSO_4(H_2O)_2]^-$ species is present on the resin, because $[UO_2Cl_2SO_4(H_2O)]^{2-}$ would easily out-compete Cl^- based on electrostatics, and there would be minimal decrease in U extraction as $[Cl^-]$ increases. We hypothesise that the drop in U extraction occurs because as chloride in solution increases, there is more available to compete with $[UO_2ClSO_4(H_2O)_2]^-$. Despite the greater affinity of the resin functional group for the $[UO_2ClSO_4(H_2O)_2]^-$ species, because the chloride ion is much smaller and more charge dense, and increases in concentration

while the U concentration remains constant, it competes effectively with $[UO_2ClSO_4(H_2O)_2]^-$ in the 1-2 M Cl^- regime. The affinity for the $[UO_2ClSO_4(H_2O)_2]^-$ species is greater than for Cl^- (explaining why there is still U extracted, albeit at a reduced percentage), but it doesn't preclude chloride uptake from occurring, especially considering that at 2 M Cl^-, the ratio of U:Cl is 1:500.

The U(VI) complex containing 1 bidentate sulfate, 1 chloride and 2 aquo ligands as represented in Figure 1c. Note that for R6, the mixed species was able to provide a goodness of fit value, R, lower than the U-*tetra*-chloro complex, but the DWFs of the mixed chloro-sulfato complex were unreasonable. It was not possible to produce a version of this complex with reasonable parameters that could provide a better fit than the U-*tetra*-chloro complex.

For all samples, a single complex provided a better fit than the linear combination. These best fit values are highlighted in grey in Table 2. As such we attribute the results to the observation of 3 different U(VI) species covering distinct salinity ranges: 0-0.5 M, 1-2 M and 3-6 M Cl^-. Given the best fitting approach for each sample as identified above in Table 2, the detailed EXAFS fits for each resin sample are presented in Tables S1, S2 and S3 in the electronic supplementary information.

3.2.2 EXAFS of U(VI) in feed solutions

Uranium L3-edge EXAFS and Fourier transforms of the EXAFS for U(VI) feed solutions, plus their corresponding fits, are shown in Figure 5, and EXAFS fits are summarized in Table S4 in the electronic supplementary information.

The EXAFS and Fourier transforms of the EXAFS for the U(VI) adsorbed resin samples (Fig. 4) can be visually compared to the spectra for the corresponding U(VI) feed solutions (Fig. 5) for a qualitative determination of whether the U species adsorbed by the resin is a direct reflection of the U species present in solution). There are significant differences in the EXAFS data between the feed solutions and resins, namely the presence of more features in the EXAFS and more distinct peaks in the Fourier transforms of the EXAFS for the resin samples. This indicates a higher degree of structure in the U(VI) species on the resin samples.

For each feed solution, the aqueous U speciation was dominated by 5-fold coordination in the equatorial plane. This is consistent with other EXAFS and DFT studies for U(VI) solution speciation [16,17,23], but in disagreement with studies on mineral processing liquors where the speciation was assumed in the absence of any spectroscopic data [12-14]. This highlights the importance of using spectroscopy and/or density functional theory when determining speciation of complex solutions.

For feed solution sample A0 (0 M $[SO_4^{2-}]$, 1 M $[Cl^-]$) the U first shell coordination environment was fitted with 2 O at 1.76 Å with DWF's, $2\sigma^2$, for these bonds fixed to 0.007 as per Hennig et al. [23]. This was done to allow a greater degree of freedom to be given over to the fitting of the second and third

shells, if necessary. The U second shell coordination environment was found to consist of 3 O at 2.25-2.42 Å, and 2 Cl at 2.63-2.74 Å with no U third shell coordination environment discernible. One relatively short equatorial oxygen distance (here O_{eq2} at 2.25 Å) is not unexpected, and may represent a hydroxyl oxygen rather than a water oxygen. Similar results were observed by Sherman et al.in their density functional theory calculations [33]. While pH 1.6 may be considered too acidic for the hydrolysis of U, recent Fourier transform infrared spectroscopy measurements identified the presence of U-OH species at much lower pH values than predicted by speciation modelling [34]. The resulting complex can therefore be described as a U-*bis*-chloro species (Fig. 2a). Our findings differ from those of Hennig et al. [23] who found only one equatorial chloride at 3 M [Cl^-]. However, the U(VI) concentration here was ~2.5 times less than that employed by Hennig et al., elevating the relative chloride concentration and possibly explaining the presence of two equatorial chlorides in our 1 M [Cl^-] feed solution.

For feed solution samples A3 and A4 (0.24 M [SO_4^{2-}], 0.5 & 1 M [Cl^-] respectively), the U first shell coordination environment consisted of 2 O at 1.78-1.80 and 1.72-1.73 Å. The U second shell coordination environment consisted of 4 O at 2.25-2.43 Å, and 1 Cl at 2.67 or 2.68 Å, and the U third shell coordination environment consisted of 1 bidentate S at 3.11 or 3.12 Å, and 1 monodentate S at 3.56 or 3.57 Å (Figure 2b). Here, the shortest second shell O distance for A3 and A4 (2.25 Å for both complexes) arise from association with the monodentate sulfate ligand [16] and the lone oxygen distances (2.29 and 2.34 Å, respectively, for A3 and A4) arise from H_2O ligands [23,33].

The range of U-O and U-Cl bond lengths in the solution samples, as well as the mixed speciation for samples A3 and A4 (with chloride and mono- and bi-dentate sulfate) is likely reflective of the fact that under the solution conditions tested, there are a variety of U species present (a combination of U-aquo, -hydroxy, -chloro, -sulfato, -*bis*-sulfato etc.) that are similar, but not identical. As EXAFS is only able to measure the average coordination environment over the measurement time, the data analysis indicates a mixture of complexes is present.

4. DISCUSSION

4.1 Change in U(VI) speciation between liquor and resin surface

The EXAFS data demonstrates that U(VI) speciation in the feed solutions differed from the species adsorbed on to the resin surface. This is especially apparent in the transition from solution species that are 5-coordinate in the equatorial plane, to the U-*tetra*-chloro resin species that is 4-coordinate in the equatorial plane. This implies there is a re-organisation of U coordination at the surface during adsorption. This is proposed to be due to a de-watering process, which would be consistent with the hydrophobic nature of the resin. This is a significant result, and is consistent with the findings of Allen et al. for U(VI) from chloride media [22]. Importantly, our results show that the reorganization of U(VI)

coordination at the surface happens in relatively low concentration media (~0.25 M [SO_4^{2-}]), as well as in heavily concentrated media (5.8 M [Cl^-]) [22]. Typically, in mineral processing circuits incorporating ion exchange, resin functionality is chosen or designed based on the assumption that the dominant solution species will be the one taken up by the resin. This study has shown that this is an incorrect assumption, and where a mixed chloride-sulfate media is concerned, a more fundamental approach examining the solution speciation should be considered.

4.2 Implications for uranium mineral processing circuits

Across the range of [Cl^-] examined, it has been shown that a weak base resin is able to adsorb three distinct U(VI) species. In the case of seawater, where the salinity is around 0.6 M, these results suggest that the U-*bis*-sulfato species will be the predominant species adsorbed by the resin. This allows for the design of an anion exchange resin with functional group chemistry that can selectively target the uptake of the U-*bis*-sulfato species, and a stripping solution chemistry that can specifically target the removal of this species.

Work to refine the most appropriate resin functionality for U(VI) extraction from sulfate mineral processing circuits incorporating seawater is an ongoing focus of our group [35], and will be the subject of forthcoming communications. Uptake of large species by Dowex Monosphere 77 can often be affected by steric hindrance due to the proximity of the tertiary amine functionality to the resin matrix. By increasing the chain lengths, it may be possible to increase the potential for chelation, and hence further improve uranium uptake in the presence of chloride. Chelation has much faster U(VI) uptake kinetics than anion exchange, but is more likely to be impacted by impurities such as iron which will preferentially chelate. The anion exchange process has better selectivity for uranium over iron but the kinetics are slower than chelation and hence larger volumes of resin are required.

In order to design targeted resin functional group chemistry and stripping solution chemistry, it is also necessary to understand the impact of contaminant ions other than chloride. Here, our synthetic liquor stream was effectively 'clean': it contained only water, sulfuric acid, uranyl sulfate and sodium chloride. In real mineral processing systems or wastewater streams, there are often many contaminant ions present. Of particular concern is Fe^{3+}, which is often present in appreciable concentrations and is known to compete with uranium for resin surface sites, especially with increasing chloride [36]. As for uranium however, there are no spectroscopic studies on the speciation of iron in mixed chloride/sulfate media, nor any concerning the mechanisms by which iron outcompetes uranium for anion exchange/chelation sites. To fully understand the mechanism by which Fe competes with U in a chloride impacted anion exchange circuit an XAS study concerning both Fe and U speciation on the resin surface

would be highly beneficial. This would allow greatly selectivity to be built into the resin functional group design, as well as into the stripping process.

5. CONCLUSIONS

- Using commercially available resins, the proportion of U(VI) extracted from acidic sulfate-based liquor streams is strongly dependent on the salinity of the liquor. For $0 \leq [Cl^-] \leq 0.5$ M leach solutions, > 95 % of U(VI) is extracted, for $0.5 \leq [Cl^-] \leq 2$ M there is a systematic decrease in U(VI) extraction to ~ 30 %, and for $[Cl^-] > 2$ M a gradual increase in U(VI) extraction to ~70 % at 5.8 M Cl^-.
- Across the salinity range 0-6 M Cl^-, 3 distinct U(VI) species are adsorbed by the weak-base anion exchange resin. These complexes have been identified as a $[UO_2(SO_4)_2H_2O]^{2-}$ (U-*bis*-sulfato) species from 0-0.5 M Cl^- solutions, a $[UO_2Cl(SO_4)_2.2H_2O]^-$ (U-chloro-sulfato) species from 1-2 M Cl^-, and a $[UO_2Cl_4]^{2-}$ (U-*tetra*-chloro) species in 3-5.8 M Cl^- solutions.
- Electrostatics appears to be the dominant factor, dictating the degree to which the uranium species are extracted. The two -2 charged U species readily outcompete Cl^- uptake, and while the tertiary amine functional groups of the resin have a greater affinity for the -1 charged U species over chloride, this does not preclude the uptake of the smaller, more charge dense Cl- ion, especially given the degree to which it outnumbers U complexes (1:500 at 2 M Cl^-).
- The predominant U(VI) species present in the liquor differ from those taken up by the resin. In order for this to occur, there must be a reorganisation of the U coordination at the surface, likely by a dewatering process. This has been identified for chloride media but not previously for sulfate media.
- Seawater has a salinity of around 0.6 M $[Cl^-]$. At this concentration the most likely U(VI) species encountered on the surface of a weak base anion exchange resin is the $[UO_2(SO_4)_2H_2O]^{2-}$. With this knowledge, it will be possible to design an anion exchange resin with functionality that has a high affinity for this species over Cl^-. Further, stripping solution chemistry could also be redesigned to preferentially strip this specific uranium species.
- EXAFS has been shown to be a powerful tool for determining both the dominant aqueous and adsorbed speciation of U in an ion exchange circuit. Here, chloride was considered as the sole 'contaminant'. This technique could also be applied to systems containing iron as an additional contaminant, determining both the influence of iron on the U speciation, but also the effect of chloride on iron speciation. This extended knowledge would allow for increased efficiency in the design of new anion exchange resins.

Acknowledgements

The authors acknowledge ANSTO Minerals for providing funding for this study, and Damian Conroy and Patrick Yee of ANSTO Minerals for conducting ICP-MS and ICP-OES analyses. We thank Karin Soldenhoff of ANSTO Minerals for providing a thorough review of this manuscript. This research was undertaken on the XAS beamline at the Australian Synchrotron, Victoria, Australia. We thank the Australian Synchrotron for providing beamtime and travel funding (M5424), and thank XAS beamline scientists Peter Kappen and Bernt Johannessen for providing beamline assistance and helpful discussion of the XAS data.

References

[1] International Atomic Energy Agency. Energy, Electricity and Nuclear Power Estimates for the Period up to 2050. International Atomic Energy Agency, Vienna, 2015.

[2] J.-Y. Yu, B. Heo, Appl. Geochem. 16 (2001) 1041-1053.

[3] C. H. Gammons, S. A. Wood, J. P. Jonas, J. P. Madison, Chem. Geol. 198 (2003) 269-288.

[4] I. Grenthe, J. Fuger, R. J. M. Konings, R. J. Lemire, A. B. Muller, C. Ngyen-Trung Cregu, H. Wanner, in: H. Wanner, I. Forest (Eds.), Chemical Thermodynamics of Uranium. OECD Publications, Paris, 2004.

[5] J. J. Pigram, Australia's Water Resources: From use to management, CSIRO Publishing, Collingwood, 2006.

[6] Government of South Australia. Assessment Report, Environmental Impact Statement: Olympic Dam Expansion, Government of South Australia, Adelaide, 2011.

[7] K. Soldenhoff, D. Wilkins, M. Shamieh, R. Ring, International symposium on the process metallurgy of uranium – URANIUM 2000, MetSoc, Saskatoon, 2000.

[8] J. E. Grindler, The Radiochemistry of uranium. National Academy of Science, Washington, D.C., 1962.

[9] Z. Zhu, Y. Pranolo, C.Y. Cheng, Proceedings of ALTA 2012 Conference on Uranium, Alta Metallurgical Services, Melbourne, 2012.

[10] M. Feinerman-Melnikova, K. Soldenhoff, CIM Journal, 3 (2012) 117-124.

[11] A. Wilson, M. Fainerman-Melnikova, K. Soldenhoff, Proceedings of ALTA 2011Conference on Uranium, Alta Metallurgical Services, Perth, 2011.

[12] A.C.Q. Ladeira, C.R. Goncalves, J. Hazard. Mater., 148 (2007) 499-504.

[13] T. Vercouter, P. Vitorge, B. Amekraz, C. Moulin, Inorg. Chem., 47 (2008) 2180-2189.

450 [14] A.N. Zagorodnyaya, Z.S. Abisheva, A.S. Sharipova, S.E. Sadykanova, Y.G. Bochevskaya, O.V.
451 Atanova, Hydrometallurgy, 131 (2013) 127-132.
452 [15] I. Billard, E. Ansoborlo, K. Apperson, S. Arpigny, M.E. Azenha, D. Birch, P. Bros, H.D. Burrows,
453 G. Choppin, L. Couston, V. Dubois, T. Fanghanel, G. Geipel, S. Hubert, J.I. Kim, T. Kimura, R. Klenze,
454 A. Kronenberg, M. Kumke, G. Lagarde, G. Lamarque, S. Lis, C. Madic, G. Meinrath, C. Moulin, R.
455 Nagaishi, D. Parker, G. Plancque, F. Schernaum, E. Simoni, S. Sinkov, C. Viallesoubranne, Appl.
456 Spectrosc., 57 (2003) 1027-1038.
457 [16] C. Hennig, K. Scheide, H. Moll, S. Tsushima, and A.C. Scheinost, Inorg. Chem. 46 (2007) 5882-
458 5892.
459 [17] V. Vallet, and I. Grenthe, C.R. Acad. Sci., Ser. IIc: Chim., 10 (2007) 905-915.
460 [18] C. Nguyen-Trung, G.M. Begun, D.A. Palmer, Inorg. Chem., 31 (1992) 5280-5287.
461 [19] H. Moll, T. Reich, C. Hennig, A. Rossberg, Z. Szabo and I. Grenthe, Radiochim. Acta, 88 (2000)
462 559-566.
463 [20] M. Gal, P.L. Goggin and J. Mink, Spectrochim. Acta, 48 (1992) 121-132.
464 [21] J. Neuefeind, S. Skanthakumar and L. Soderholm, Inorg. Chem., 43 (2004) 2422-2426.
465 [22] P.G. Allen, J.J. Bucher, D.K. Shuh, N.M. Edelstein, N.M. and T. Reich, Inorg. Chem. 36 (1997)
466 4676-4683.
467 [23] C. Hennig, J. Tutschku, A. Rossberg, G. Berhard and A.C. Scheinost, Inorg. Chem., 44 (2005) 6655-
468 6661.
469 [24] C.E. Harland, Ion Exchange: Theory and Practice, 2nd ed. Royal Society of Chemistry, Cambridge,
470 1994.
471 [25] K. V. Klementiev, J. Phys. D: Appl. Phys., 34 (2001) 209-17.
472 [26] A. Tenderholt, B. Hedman, and K.O. Hodgson, AIP Conf. Proc. (XAFS13), 882 (2007) 105-107.
473 [27] N. Binsted, EXCURV98: The Manual, CLRC Daresbury Laboratory, Warrington, 1998.
474 [28] L. Hedin and S. Lundqvist, Solid-State Phys., 23 (1970) 1–181.
475 [29] E.A. Stern, Phys. Rev. B, 48 (1993) 9825-9827.
476 [30] C.H. Booth and Y.-J. Hu, J. Phys. Conf. Ser., 190 (2009) 1-6.
477 [31] N. Binsted, M.J. Pack, M.T. Weller and J. Evans, J. Am. Chem. Soc., 118 (1996) 10200-10210.
478 [32] M. Walther, T. Arnold, T. Reich, G. Bernhard, Environ. Sci. Technol. 37 (2003) 2898-2904.
479 [33] D. M. Sherman, C. L. Peacock, C. G. Hubbard, Geochim. Cosmochim. Acta, 72 (2008) 298-310.
480 [34] K. Muller, V. Brendler, H. Foerstendorf, Inorg. Chem., 47 (2008) 10127-10134.
481 [35] M.D. Ogden, E.M. Moon, A. Wilson, S.E. Pepper, Chem. Eng. J. (2017) In press,
482 http://dx.doi.org/10.1016/j.cej.2017.02.041

[36] A.C.Q. Ladeira and L.C. Sicupira, Proceedings of the 13th International Conference of Environmental Science and Technology, Athens, Greece, 2013.

Tables

Table 1

Parameter	Value	
Total exchange capacity	1.7	1.57[b]
Weak base capacity	1.5	1.32[b]
Commercial equivalent	Purolite , Lewatit	
Particle size	475 – 600 μm[a]	
Functionality	Tertiary amine	
Form	Free base	
Moisture	40 - 50%	

[a] – Volume median diameter

[b] –Experimentally determined via Harland method [24]

Table 1 - Manufacturer specifications of weak base anion exchange resin Dowex Monosphere 77

Table 2

Sample	U-*bis*-sulfato complex	U-*tetra*-chloro complex	Mixed complex	Linear Combination		
	Fit (R)	Fit (R)	Fit (R)	Fit (R)	% R1	% R7
R1	25.8	-	-	-	-	-
R2	23.4	47.2	24.7	26.2	99	1
R3	21.0	43.7	22.8	26.3	89	11
R4	28.2	29.2	20.7	26.1	51	49
R5	38.6	25.4	20.4	25.9	34	66
R6	46.0	26.0	N/A*	30.1	26	74
R7	-	17.6	-	-	-	-

*N/A indicates that the complex could not produce a fit with reasonable parameters

Table 2 – Summary of different EXAFS fitting approaches for the resin samples presented in terms of the goodness of fit parameter (R) for each sample. The best fitting approach (i.e. lowest goodness of fit value) for each sample spectrum is highlighted in grey.

Figure Captions:

Figure 1 - Best fitting U(VI) complexes for resin samples. a) U-*bis*-sulfato species $[UO_2(SO_4)_2.H_2O]^{2-}$, b) U-*tetra*-chloro species $[UO_2Cl_4]^{2-}$ c) a mixed U-chloro-sulfato species $[UO_2(SO_4)Cl.2H_2O]^{-}$. Dashed atoms were not included in the fit, but are displayed for clarity.

Figure 2 - Best fitting U(VI) complexes for feed solution samples. a) U-*bis*-chloro species $[UO_2Cl_2(OH)_2.H_2O]^{2-}$, b) U-chloro-*bis*-sulfato species $[UO_2Cl(SO_4)_2(OH)]^{4-}$. Dashed atoms were not included in the fit, but are displayed for clarity.

Figure 3 -Uranium extraction from a sulfate-based mineral processing liquor by a weak-base anion exchange resin, Dowex Monosphere 77 ([U(VI)] = 0.004 M, $[SO_4^{2-}]$ = 0.24 M, pH 1.6, 21ºC, 24 h contact time, resin functional group = tertiary amine).

Figure 4 - EXAFS and Fourier transform of EXAFS for U(VI) speciation on the IX resin surface. Solid lines are data, dotted lines are fits.

Figure 5 – EXAFS and Fourier transform of EXAFS for U(VI) speciation in the feed solutions. Solid lines are data, dotted lines are fits.

526 **Figures**

527

528 Figure 1 (1 column wide - colour)

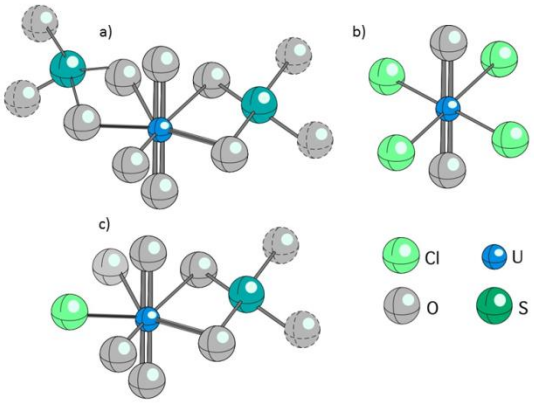

529

530

531 Figure 2 (1 column wide - colour)

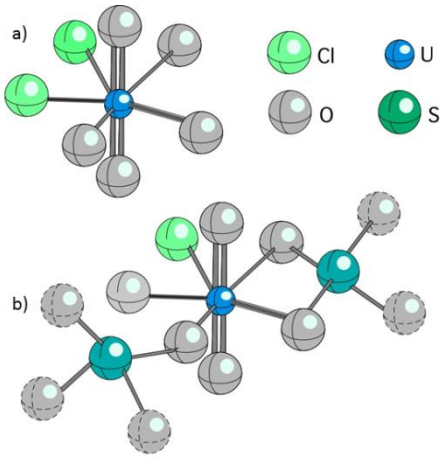

532

533

534 Figure 3 (1 column wide – black and white)

535

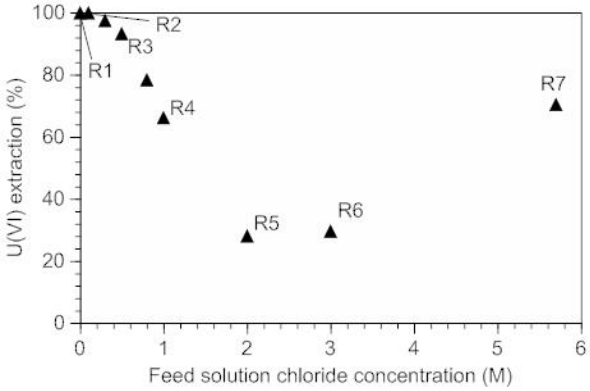

536

537

538

539 Figure 4 (2 columns wide – black and white)

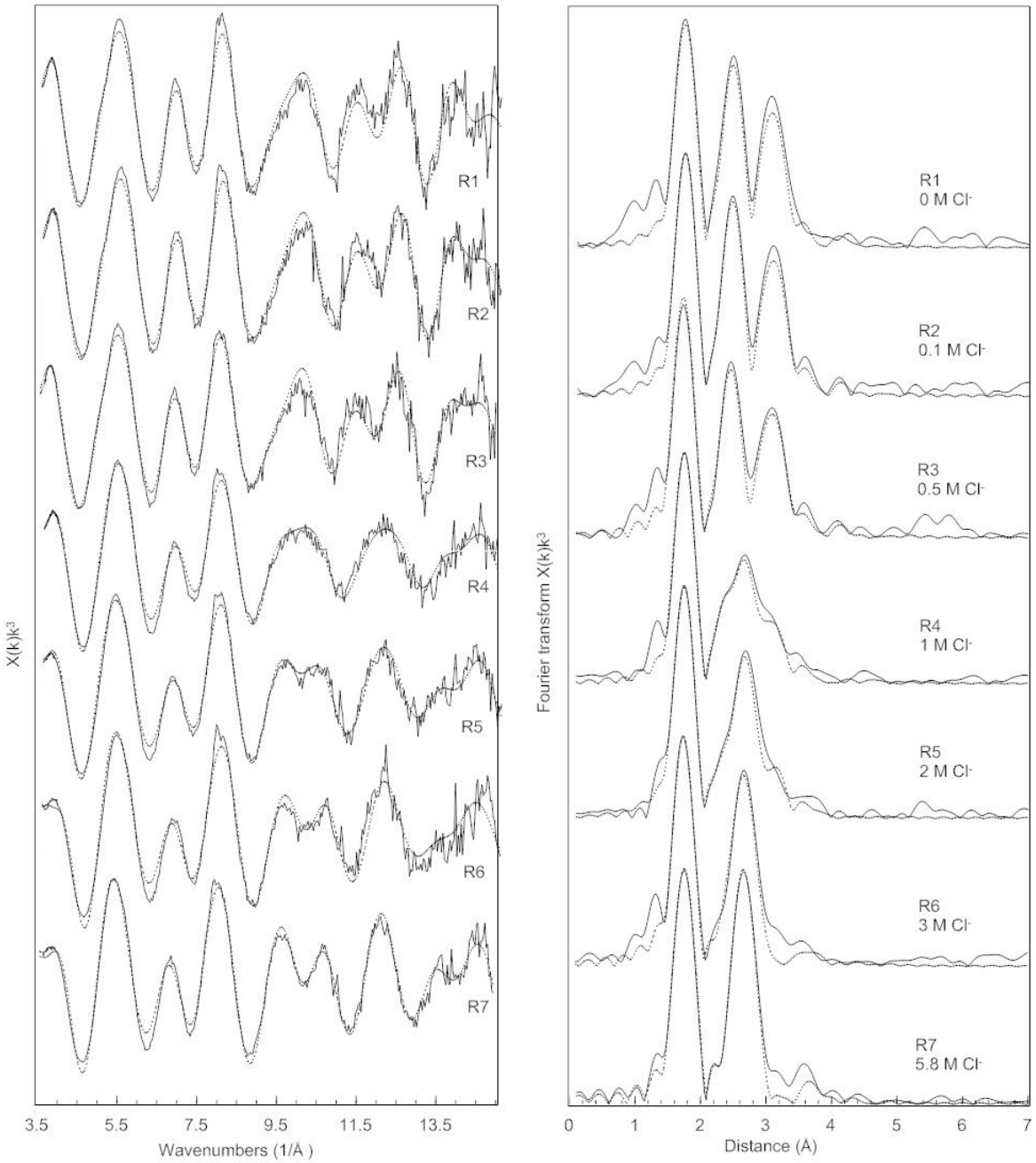

540

541

542

543

544

545

546 Figure 5 (2 columns wide – black and white)

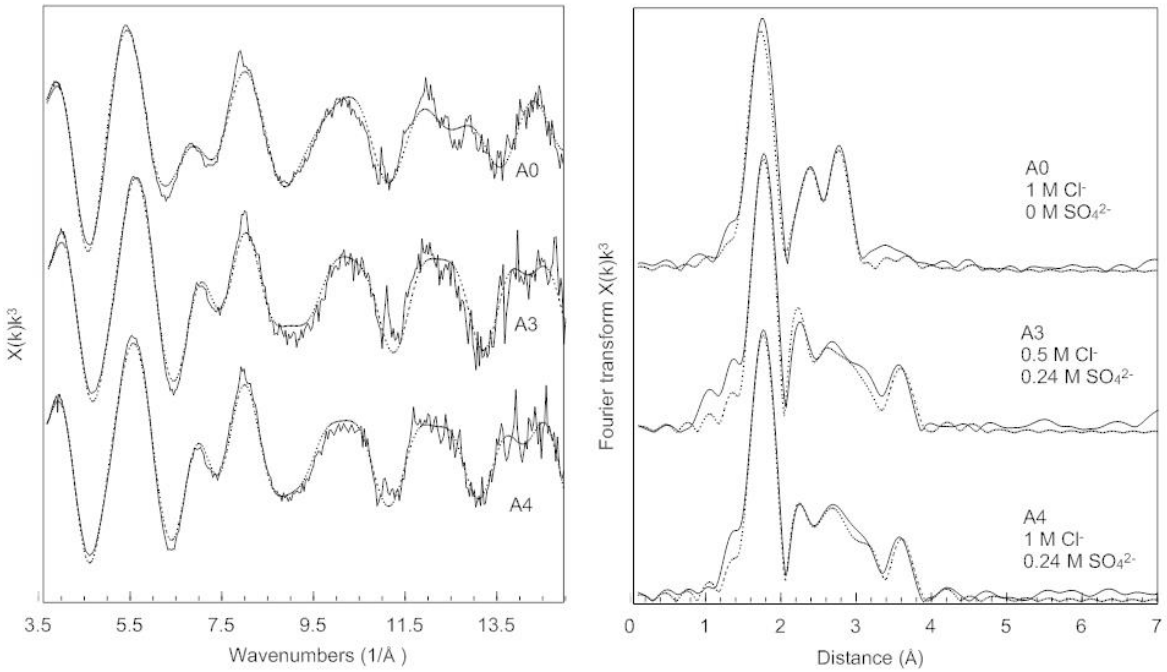

547

548

549

550